Experimental Investigation on the Performance of Radial Flow Desiccant Bed Using Activated Alumina

دراسة تجريبية حول أداء مهد مجفف ذي سريان قطري يعمل باستخدام الألومينا المنشطة

W. R. Abd-Elrahman, A. M. Hamed, S. H. El-Emam and M. M. Awad

Mechanical Power Engineering Department, Faculty of Engineering, Mansoura University, El-Mansoura, Egypt.

خلاصة في هذا البحث تم عرض نتائج دراسة تجريبية عن أداء مهد مجفف ذي سريان قطري يعمل باستخدام الألومينا المنشطة. تم استخدام ٣٩,٨٦ كجم من حبيبات الألومينا بقطر متوسط قدره ٤ مم داخل المجفف لتكون مهدا على شكل أسطوانة مجوفة بطول ٩٠ سم وقطر خارجي ٢٧,٨ سم وداخلي ١٠,٨ سم ، للحصول على سريان قطري للهواء المار داخل المجفف. في هذه الدراسة تم استخدام وسيلة دقيقة تتمثل في خلية قياس وزن لبيان مقدار التغير اللحظي في وزن المهد مع الزمن وبالتالي تقدير ما يتم امتصاصه أو فقده من الماء أثناء عمليتي الامتصاص أو التنشيط للمهد على الترتيب. أجريت الدراسة عند ظروف مختلفة للهواء عند الدخول وأيضا عند قيم مختلفة لدرجات الحرارة والمحتوى المائي للمهد قبل التشغيل. وقد تم قياس كل من درجة الحرارة والرطوبة للهواء الداخل إلى المجفف وأيضا عند الخروج منه عند ظروف التشغيل المختلفة. تم توقيع نتائج القياس على الخريطة السيكرومترية لبيان التغير في حالة الهواء وتحديد أداء المجفف. وقد تم التركيز على دراسة تأثير التبريد المسبق للمهد على الامتصاص حيث أوضحت النتائج أن هذا التبريد والذي يتم طبيعيا بين المهد والجو المحيط به له تأثير واضح على حالة الهواء الخارج من المهد. وقد أوضحت النتائج أنه تم خفض رطوبة الهواء من قيم تتراوح بين ١٨,٧ إلى ١٢,٥ جم/كجم عند دخوله إلى المهد لتصل الى ١,٢ جم/كجم عند الخروج منه وذلك عندما كانت كل من درجة حرارة المهد الابتدائية ودرجة حرارة الهواء الداخل ٣٢,٥ °م .

Abstract In the present work, an experimental investigation on the performance of radial flow desiccant bed using activated alumina has been carried out. A weight of 39.860 kg of spherical particles of the activated alumina with an average diameter of 4mm is used to form a hollow cylindrical shape bed with length of 90 cm and outer and inner diameters of 27.8 and 10.8 cm, respectively, to obtain radial flow of the air through the bed. In the present study, the weight of the bed is measured instantaneously using an accurate load cell to determine the adsorbed and desorbed water during the adsorption and desorption processes, respectively. The experimental tests are carried out at different inlet air and initial bed conditions. Values of temperature and humidity of the air at inlet and exit of the bed are measured. Air inlet, and exit conditions are plotted on the psychrometric chart to demonstrate the transient variation of air conditions and the bed performance. In this study, effect of bed pre-cooling on the system performance is highlighted. The obtained results show that air with inlet humidity ranging from 18.7 to 12.5 g/kg could be dehumidified, using activated alumina, to a lower level of humidity (1.2 g/kg) when the temperature of the inlet air and bed temperature equal 32.5 °C.

Keywords: Desiccant, activated alumina, adsorption, air conditioning.

Nomenclature

A	Area , m^2	RH	Relative humidity
$\dot{m}_a$	Mass flow of dry air, kg/s	T	Temperature, °C
M_{ads}	Adsorbed mass, kg	v	Air flow velocity, m/sec
$\dot{M}_{ads}$	Adsorption rate, kg/s	X	Bed water content, kg/kg dry alumina
P	Pressure, N/m^2	W	Bed weight

Accepted June 30, 2010.

Greek symbols	
Δ	Difference
ρ	Density, kg/m^3
τ	Time, s
ω	Humidity ratio, g/ kg dry air
Superscripts	
*	At equilibrium with bed condition
Subscripts	
a	Air
ads	Adsorbed
amt	Atmosphere air
b	Bed
d	Dry bulb
e	Exit
i	Inlet
L_cell	Load cell
reg	Regeneration
sat	Saturation
v	Vapor
w	Wet bulb

1- Introduction

Air dehumidification can be achieved by two methods: cooling the air below its dew point and removing moisture by condensation or by a sorption process through desiccant material. Desiccants in either solid or liquid forms have a natural affinity for removing moisture. As the desiccant removes the moisture from the air, it releases heat and warms the air, i.e., latent heat becomes sensible heat. The dried warm air can then be cooled to the desired comfort conditions by sensible coolers (e.g., evaporator coils, heat exchangers, or evaporative coolers.). To re-use the desiccant, it must be regenerated or reactivated through a process in which moisture is driven off by heat from an energy source such as electricity, waste heat, natural gas, or solar energy, Pesaran (1993).

The design and operation of a desiccant system are based on the desiccant material used to accomplish the dehumidification. Desiccant materials attract moisture through the process of either adsorption or absorption. Adsorption is the process of trapping moisture within the desiccant material similar to the way a sponge holds water through capillaries. Most adsorbents are solid materials. Absorption is the process of trapping moisture through a chemical process in which the desiccant undergoes a chemical change. Most absorbents are liquids. Types of materials used as a basis for desiccant systems are given by Rutherford (2000).

Solid desiccant cooling and dehumidification systems have received considerable attention in the past several years as alternatives or supplements to conventional vapor compression machines for air conditioning of buildings and spaces that have high latent loads (Pesaran and Bingham, 1989).

Theoretical and experimental study on the transient adsorption characteristics of vertical packed porous bed was carried out by Hamed (2002). He investigated a theoretical model to describe the effect of independent parameters (time, and vertical distance) on the vertical gradient of adsorbable fluid in a desiccant bed.

Hamed *et al.* (2010) studied experimentally the transient adsorption/desorption characteristics of solid desiccant in a vertical fluidized bed. They found that, the relation between the adsorbed water and the moisture fraction for material depends on the thermophysical properties of the solid adsorbate-adsorbent pair. In silica gel the relation can be expressed as a linear function. They carried out a comparison test between packed and fluidized bed adsorption. The test result showed that in lower the exit air humidity case, the performance of the bed under fluidization condition is better than packed one. On the other hand, accumulation of the heat of adsorption in packed bed results in increase in the bed temperature when compared with that of fluidized bed.

Kabeel (2009) studied the effect of design and operating parameters on the performance of a multilayer desiccant packed bed theoretically and experimentally. He compared his experi-

mental and theoretical results with that of Abd-Elrahman (2005), and the comprised results showed reasonable agreement.

Awad *et al.* (2008) attempted to improve the performance of a packed bed dehumidifier. Where, a radial flow hollow cylinder packed bed had been investigated, as they expected, the pressure drop in hollow cylinder bed was too small compared with that in the vertical packed bed.

From the literature review, it can be found that the transient operation of the desiccant air conditioning systems need excessive experimental investigation to assess the performance of such systems when operates at variable air outlet parameters. Air parameters at the exit of the desiccant bed, however, plays decisive role in the operation and control of the different units of the air conditioning system.

The objective of the present study is to investigate the performance of radial flow hollow cylindrical packed bed dehumidifier in the transient operation. Activated alumina will be applied as the working desiccant. The isotherms of activated alumina are given in the Appendix. Experimental data are used to evaluate the conditions of the supply air at system exit and measure how far the bed output from the comfort zone. This will be a guide to built desiccant cooling system for air conditioning applications utilizing the hollow cylindrical packed bed dehumidifier using granular activated alumina as a desiccant.

2-Experimental Arrangement

2.1 Experimental Set-up

Experimental arrangements for the adsorbing and desorbing flow direction modes are shown in Fig. 1 (a) & (b), respectively. The experimental system has been fabricated, built and tested in Eldelta Company for Fertilizers and Chemical Industries at Talkha, Dakahlia, Egypt. The system has been designed to operate the desiccant bed in the adsorption and desorption modes. Air flow directions are illustrated for the two modes as shown in the figures. Air is blown to the system using air blower. Air heater is connected through a bypass between the blower and the desiccant bed for desiccant regeneration. The system piping and control valves arrangements are designed to facilitate the operation of the adsorption and regeneration modes properly.

A radial type air blower of 0.75 kW is used to provide the required air flow rates. To control the inlet air conditions (humidity and temperature), a small steamer and an electrical heater are located on the suction line near the blower inlet section (not shown in the figure).

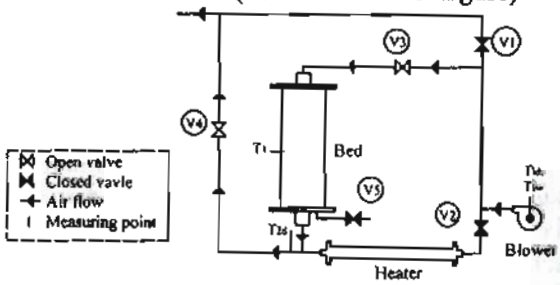

(a) Adsorbing mode

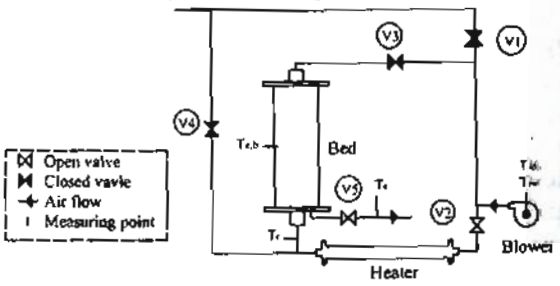

(b) Desorbing mode

Fig. 1. Experimental arrangements for the adsorbing and desorbing flow direction modes.

An electrical air heater consists of six coils connected in parallel is used for air heating during the desorption mode. Coils are suspended by ceramic pieces tightened in 100×34 cm aluminum sheet as shown in Fig. 2. The heater is enclosed by a cover case of about 10 cm diameter. The electrical heater terminals exit from a fiber disk.

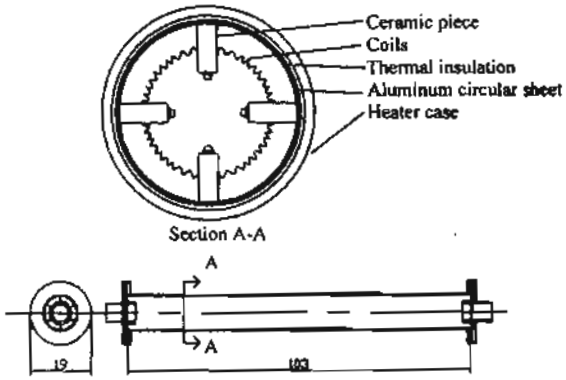

Fig. 2. A schematic diagram of the electrical heater (dimensions in cm).

The components of the desiccant adsorber are the desiccant bed, bed container and bed external case. The desiccant bed is a hollow cylindrical packed bed. Activated alumina particles with an average diameter of 4 mm fill the hollow cylindrical screen. Dimensions of the hollow cylinder packed bed are given in Fig. 3. Details of the desiccant adsorber are shown in Fig. 4. The bed container was designed to be as light as possible and its weight is 5.970 kg. The inner and the outer surface of the container are manufactured from metallic screen. The screen permits the air to move freely through the desiccant. The upper end of the central stud is used for bed lifting to execute the required measurements of bed weight using the load cell. The bed external case is a cylindrical tube of 34 cm in diameter and 101 cm length. The bed external case stands vertically on three legs. For instantaneous measurements of bed weight during adsorption and regeneration, a load cell is connected to the case from the upper surface such that the bed is freely suspended during experiments.

2-2. Instrumentation and Measurements

Measuring data which are required for analysis of the system performance include the bed weight, temperature, humidity and velocity. The weight of the bed is measured instantaneously using an accurate "S" shape load cell type. Fig. 4. illustrates details of the desiccant adsorber load cell connection mechanism. This connection allows measuring bed weight during the experiments and recording the loss or increase in weight during regeneration or adsorption processes, respectively. Rotating the lift nut clockwise will make the lifting bolt moves upward and consequently the bed now is loading by the cell freely, as shown in Fig. 5 b. Inversely, rotating the nut counter clockwise will make the bed rest on its seat again and the leakage nut and its gasket will prevent air leakage, as shown in Fig. 5 a.

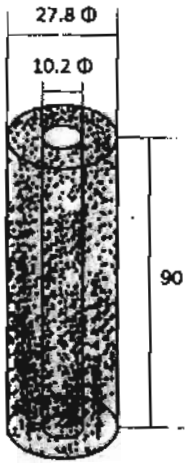

Fig. 3. Dimensions of the hollow cylinder packed bed in cm.

Two kinds of temperatures sensing probe are used in this study. RTD (BT100) and "J" type thermocouples. The temperature indicator which uses the BT 100 probes can read the temperature from -19.9 to 99.9 °C with a resolution of 0.1. While the temperature indicator for "J" type thermocouple can read temperature from 0 to 800 °C. All temperature probes are connected to a multi switch temperatures indicator. An anemometer with a measuring range of 0.7 to 25 m/s, of accuracy ± 2% and resolution of 0.01% is used to measure air velocities.

3- Analysis of Measurements

From the measured data, mass of adsorbed water is evaluated from the measured mass of

the bed and the air parameters. The adsorbed water and actual increase in bed weight are evaluated as given below and locations of measuring points are shown in Fig. 1 a.

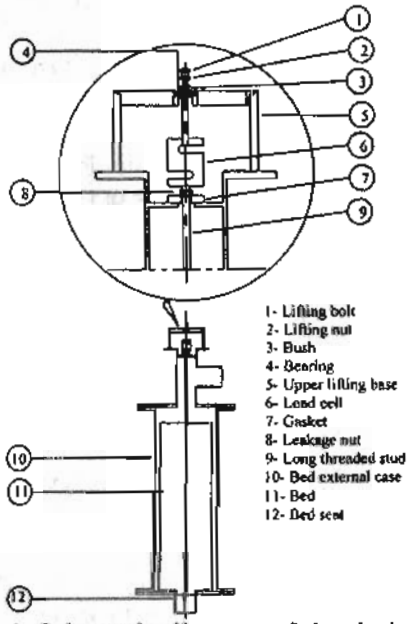

Fig. 4. Schematic diagram of the desiccant adsorber.

From the measured air inlet dry and wet bulb temperatures, $T_{i,d}$ and $T_{i,w}$ the specific humidity of air at bed inlet; ω_i can be calculated.

From air conditions at bed exit, $T_{2,d}$ and $T_{2,w}$, values of specific humidity are calculated and density of air at bed exit; ω_2, ρ_2 can be obtained. These parameters are evaluated using the psychrometric data of the air (Psychrometric charts PROFESSIONAL Edition version 3.1.7, 2002).

The rate of adsorption, $\dot{M}_{ads}$ is evaluated from;

$$\dot{M}_{ads} = (A_2 . v_2) \cdot \rho_{a,2} \cdot (\omega_i - \omega_2) \quad (1)$$

The increase of the bed mass in time in a time interval $\Delta\tau$, ΔM_{ads} can be obtained from the following relation;

$$\Delta M_{ads} = \dot{M}_{ads} \cdot \Delta\tau \quad (2)$$

The total increase in bed weight, M_{ads}

$$M_{ads} = \sum \Delta M_{ads} \quad (3)$$

The relative error can be calculated using the following relation:

$$Error = \frac{M_{ads} - \Delta W_{L\_cell}}{\Delta W_{L\_cell}} \quad (4)$$

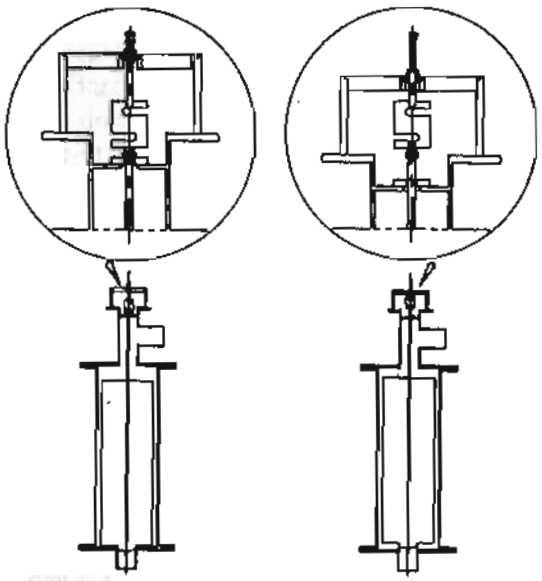

(a) the bed is rested on its seat (b) The bed is lifted by the lifting nut

Fig. 5. Schematic diagrams of the bed position.

4- Results and Discussion

4.1 Desorption Mode

Three main parameters affect the bed regeneration process. These parameters are regeneration temperature, regeneration time and flow rate of regeneration air. Table 1. shows bed and flow conditions for the carried out experiments. Comparison between the calculated mass of water which is adsorbed from the inlet air and that measured by load cell is illustrated in Table 2. It can be observed that the difference between the calculated and measured values varies from 5% to 21%. This difference may be due to expected errors in temperature, humidity and air flow rate. Instantaneous values of bed weight,

regeneration temperature and air exit temperature from the bed are depicted in Fig. 6.

Summary of the test results during regeneration mode is presented in Table 3. Analysis of test results shows that an increase in regeneration temperature increases the mass of water regenerated from the bed (see results of tests 8R and 9R). On the other hand, the regeneration air flow rate has a significant effect on regeneration rate. This result can be observed from the comparison of the results of tests 1R and 4R.

Table 1. Range of operating conditions.

Condition	Adsorption	Regeneration
Air flow rate, L/min	1458 to 2232	1951 to 2118
Air inlet temperature, °C	29.0 to 34.5	110 to 198
Air inlet humidity, g/kg	12.5 to 19.1	
Bed initial mass, kg	39.86 to 40.37	48.145 to 47.230
Number of runs	13	9

Table 2. Relative error of the calculated adsorbed water to the actual weight for the selected tests.

Test No	Bed weights (kg), by load cell			Calculated M_{ads}	*Relative Error*
	Initial	Final	Diff.		
1	45.730	46.960	1.230	1.293	+5.0
2	45.860	46.940	1.080	0.852	-21.0
3	45.830	46.810	0.980	1.023	+4.4
4	45.895	47.225	1.330	1.228	-7.8
5	45.885	47.390	1.505	1.330	-11.7
6	45.915	47.250	1.335	1.163	-12.9
7	45.890	47.330	1.440	1.222	-15.0
8	45.835	48.145	2.310	2.041	-18.0
9	46.335	47.970	1.635	1.441	-12.0
10	46.240	47.470	1.230	1.058	-14.0
11	45.910	47.580	1.665	1.549	-7.0
12	45.955	47.660	1.705	1.473	-14.0
13	45.910	47.920	2.010	1.697	-16.0

4.2 Adsorption Mode

Table 4. summarizes pertinent parameters of all adsorption tests. Experimental readings for the selected adsorption tests are presented in Figs. 7, 8 and 9. The adsorption rate is dependent on the mass transfer potential, which is the difference in vapor pressure on the bed surface and in the flowing air. The vapor pressure on the bed surface increases with increase in bed temperature. To investigate the effect of bed surface temperature on the rate of adsorption, the adsorption is carried out at different bed temperatures by allowing the bed to cool naturally after regeneration ends. After regeneration of the bed, it is left for a pre-cooling time then, the adsorption test begins. Pre-cooling time for every test is given in Table 4. The effect of bed pre-cooling for selected group of experiments is given in Table 5. Tests 4, 5 and 13 are examples of the long period of pre-cooling, whereas tests 7, 9 and 10 represents the short pre-cooling before adsorption.

Table 3. Bed and flow conditions for regeneration experiments.

Test no.	Avg. T_{reg} (°C)	Hot $\dot{m}_a$ (kg/s)	Duration time (min)	Total bed weight & desorbed mass ‡		
				Initial (kg)	Final (kg)	Desorbed mass (kg)
1R	183	0.0360	55	47.230	45.885	1.345
2R	189	0.0364	52	47.390	45.865	1.525
3R	198	0.0367	60	47.410	45.835	1.575
4R	181	0.0400	35	47.970	46.465	1.505
5R	174	0.0402	45	48.145	46.336	1.810
6R	178	0.0375	60	47.470	45.910	1.560
7R	172	0.0384	60	47.660	45.935	1.725
8R	110	0.0403	120	47.920	46.375	1.545
9R	189	0.0395	60	47.995	45.930	2.065

‡ Total bed weight = Bed weight + Bed container weight (5.970 kg)

Fig. 7 depicts the transient variation of temperatures at bed inlet and exit. It can be observed for long pre-cooling time tests that the bed temperature rises from a minimum value, which is nearly equal to the inlet temperature, to a maximum value after approximately 30 min from the start. Then, the temperature decreases gradually with the time. This can be explained as follows: when the adsorption starts, bed temperature has its lower value and consequently, the vapor pressure difference between air stream and bed surface is maximum. The adsorption heat rises the bed temperature. Subsequent increases in bed temperature results in increase in vapor pressure on the bed surface and consequently decrease in mass transfer potential. As the vapor transfer from air decreases, the rate adsorption heat

generation also decreases. Also, the flowing air cools the heated bed contentiously.

Table 4. Summary of adsorption tests.

Test no	Inlet conditions		Initial total bed weights (kg)	Pre-cooling Time (h)	Duration time (min)
	DBT (°C)	ω (g/kg)			
1	31.5	12.50	45.730	24	60
2	28.0	15.77	45.860	24	45
3	34.5	13.60	45.830	24	60
4	34.0	16.80	45.895	24	60
5	33.0	20.00	45.885	24	60
6	32.0	16.21	45.915	24	60
7	30.0	18.70	45.890	4	60
8	29.0	18.50	45.835	1½	120
9	29.0	18.50	46.335	1½	90
10	29.0	19.10	46.240	¾	60
11	28.0	16.20	45.910	½	95
12	33.0	16.20	45.955	1	100
13	32.5	14.43	45.910	24	120

Table 5. Effect of bed pre-cooling on the bed performance during adsorption.

	Long pre-cooling tests			Short pre-cooling tests		
	Test (4)	Test (5)	Test (13)	Test (7)	Test (9)	Test (10)
Pre-cooling Time (h)	24	24	24	4	1½	¾
Initial ω_o (g/kg)	2.0	2.5	1.4	2.7	7.6	7.7
Duration (min)	60	60	120	60	90	60
Final ω_o (g/kg)	9.1	11.5	10.8	9.8	12.4	10.9
Final ω_o After 1h	9.1	11.5	7.4	9.8	10.6	10.9

The instantaneous variations of exit air humidity for long pre-cooling time tests (test No. 4, 5 and 13) are represented in Fig. 8. Analysis of the measured values of humidity shows that the maximum rates of vapor transfer on the bed occurs during the starting period of adsorption. As the water content in the bed increase with the time the vapor pressure on the surface of the activated alumina particles also increase and the potential for mass transfer decrease.

The instantaneous variations of exit air humidity for short pre-cooling time tests (test No. 7, 9 and 10) are represented in Fig. 9. The variation in exit humidity from the start for short pre-cooling test is lower than that of long pre-cooling time. For example as shown in Table 5. and Fig. 9. for tests (9) and (10), the variations in exit humidity from the start up to 60 min are 3.0 and 2.2 g/kg, respectively, and that of tests (4) and (5) are 7.1 and 9.0 g/kg, respectively.

Psychrometric chart representation for the selected tests are represented in Figs. 10, 11 and 12. In the chart the comfort zone shown and the air instantaneous exit conditions are plotted. It can be noted that the air conditions at bed exit is variable. The difference between the air exit variables (temperature and humidity) depends on many parameters such as the bed initial temperature, humidity of air at bed inlet, air initial temperature, the adsorption period and the pre-cooling of the bed. For continuous operation of desiccant air conditioning system, it is essential to select the design parameters of the system and the method of control. On the other hand, the hybrid system with suitable control may be the best option for better performance of such systems.

5- Conclusions

Desiccant dehumidification system of hollow cylinder type is designed, built and tested. Experimental results of the instantaneous variation of the air exit parameters (humidity and temperature) are demonstrated.

The measurements obtained from the specific tests carried out on desiccant dehumidification system of hollow cylinder type using activated alumina as the working desiccant have been analyzed and highlighted. From the analysis, the following conclusions can be drawn.

1- Regenerated desiccant bed (activated alumina) of hollow cylinder type with weight of 39.930 kg can adsorb 2.310 kg of water vapor from humid air flowing at 0.03 kg/s and has the following psychrometric properties (T_d = 29.0 °C and ω = 18.5 g/kg).

2- For the specified design condition, air temperature of 189 °C is a proposed regeneration temperature for 1 h duration time with 0.0395 kg/s flow rate.

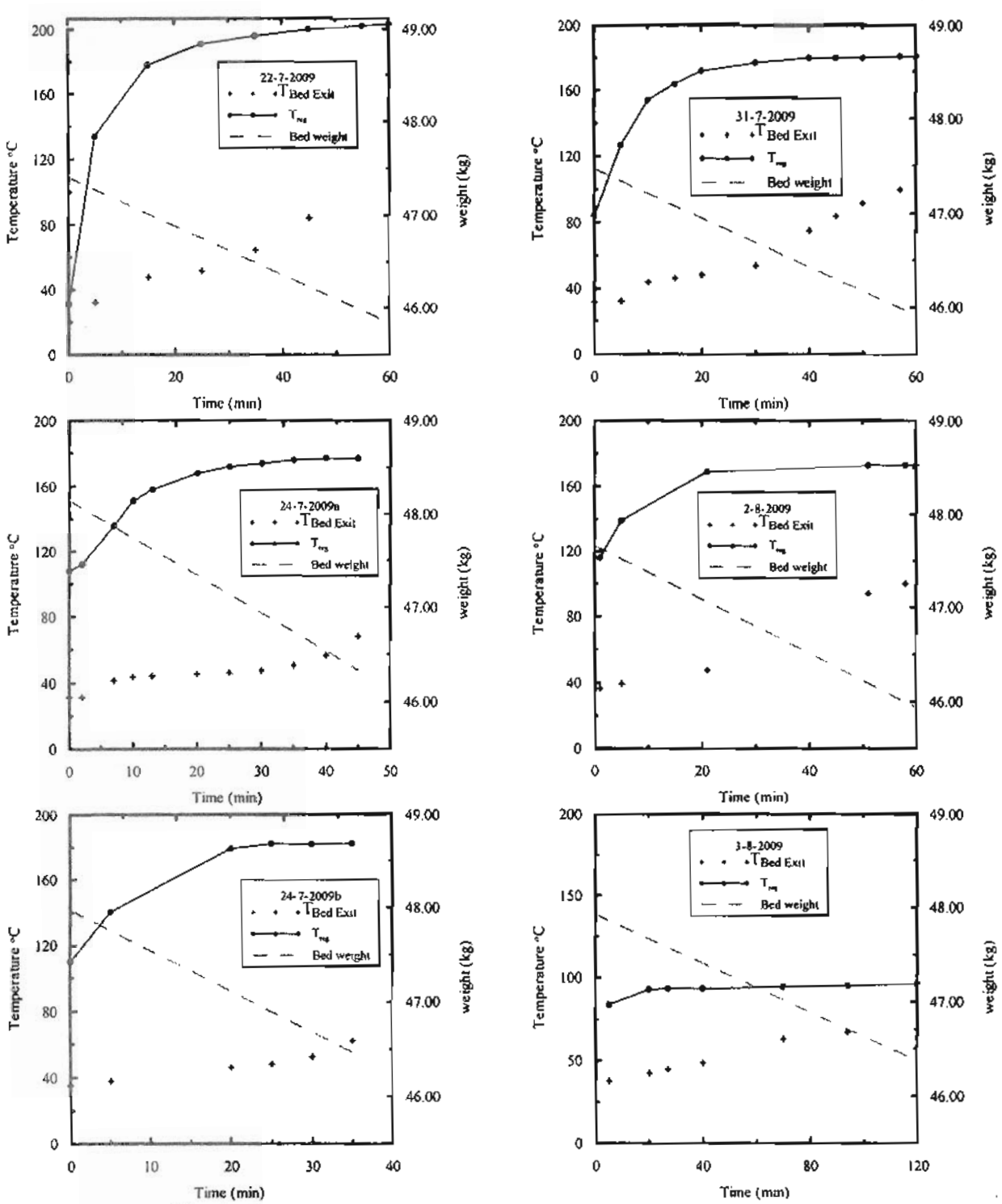

Fig. 6. Temperatures and total bed weight for the regeneration tests.

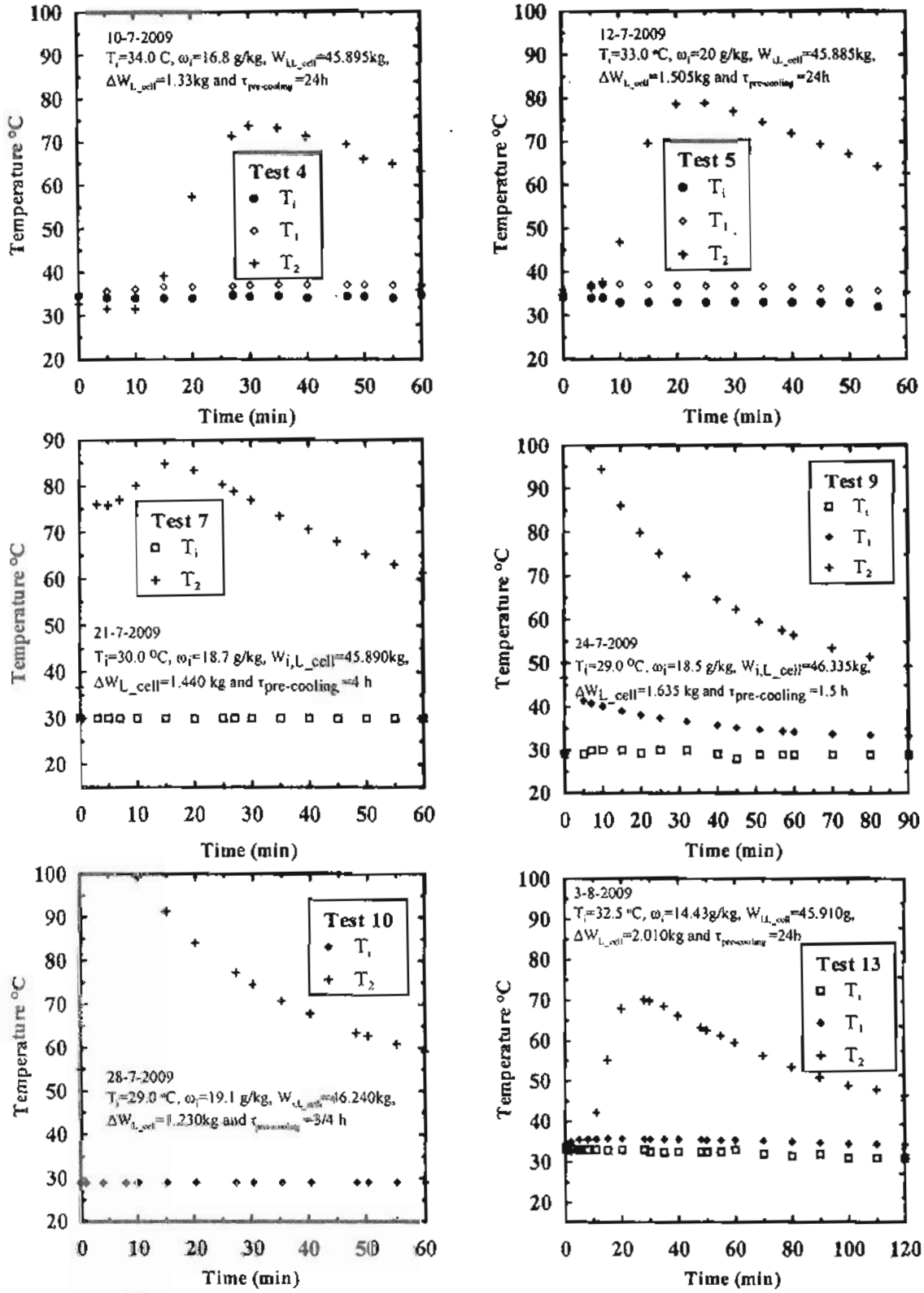

Fig. 7. Inlet and exit temperatures for the system in adsorption mode.

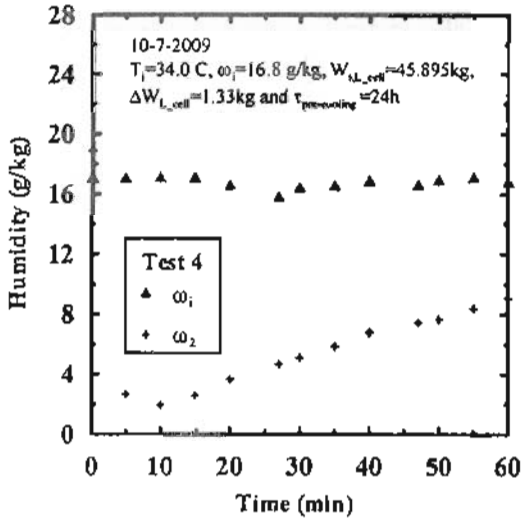

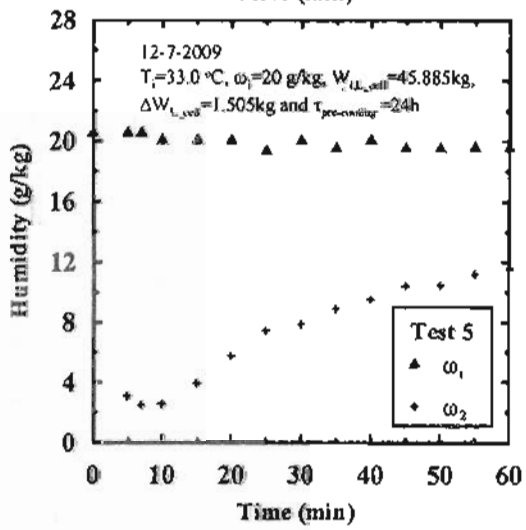

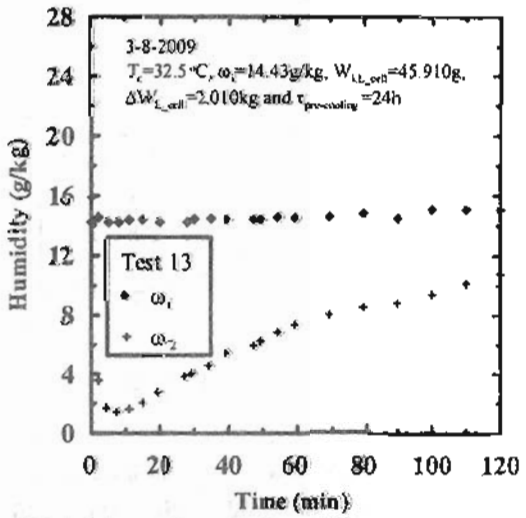

Fig. 8. Inlet and exit humidity of air in adsorption mode for long pre-cooling tests.

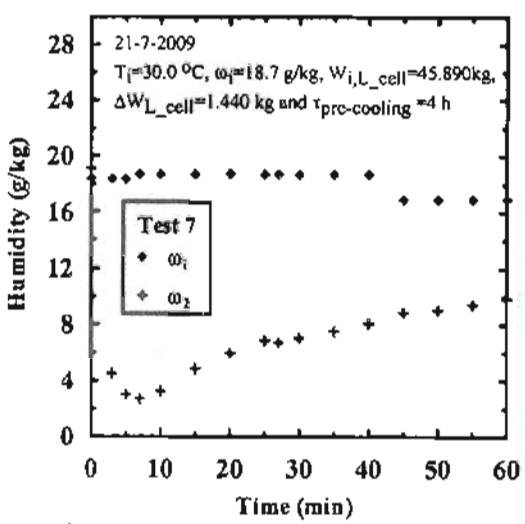

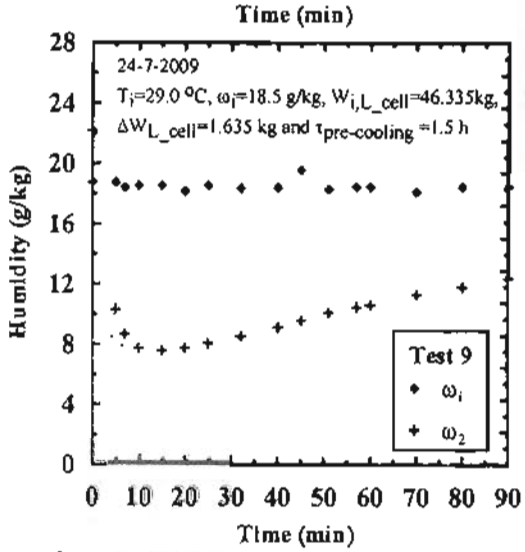

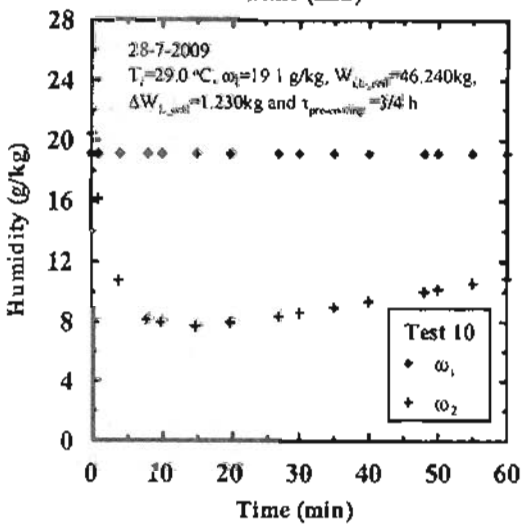

Fig. 9. Inlet and exit humidity of air in adsorption mode for short pre-cooling tests.

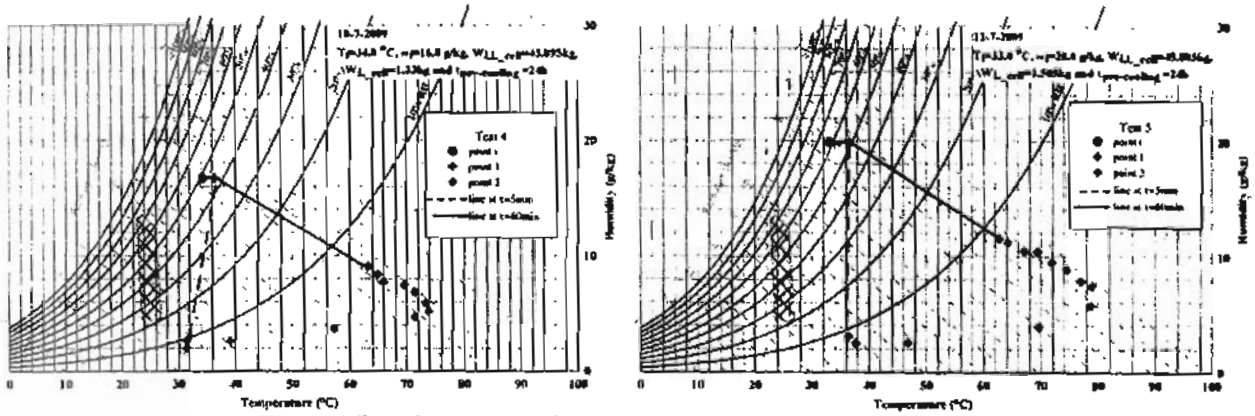

Fig. 10. Psychrometric chart representation for tests 4 and 5.

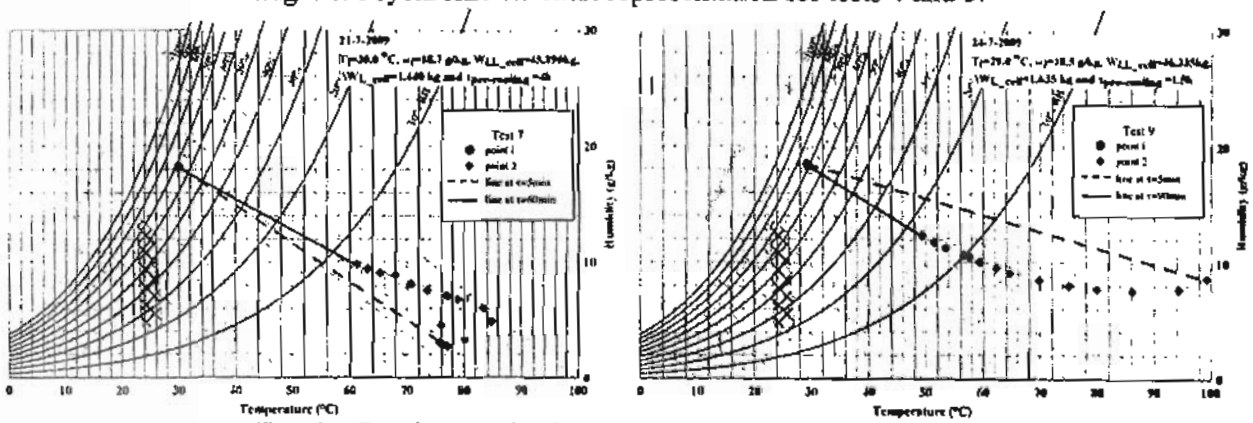

Fig. 11. Psychrometric chart representation for tests 7 and 9.

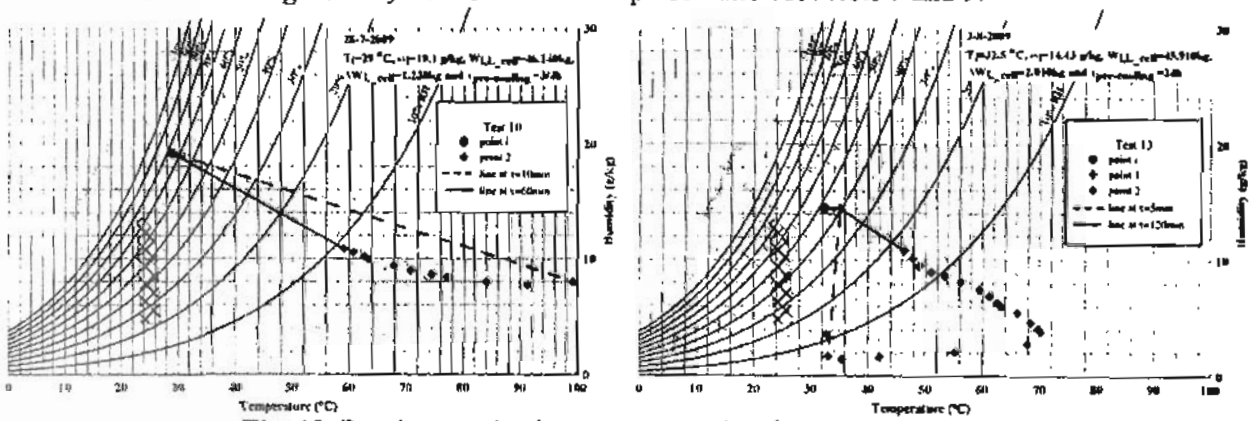

Fig. 12. Psychrometric chart representation for tests 10 and 13.

3- The variation in the exit humidity from the desiccant bed for short pre-cooling time tests is lower than that of long pre-cooling time. This is an advantage for the application which requires a specific range of air humidity.

6- References

Abd-Elrahman, W. R. (2005) "Theoretical and Experimental Study on the Performance of a Fluidized Air Dryer," M.Sc. Thesis. Mechanical Engineering Department, Mansoura University, Egypt.

Awad, M. M., Ramzy A. K. Hamed A. M. and Bekheit M. M. (2008) "Theoretical and Experimental Investigation on the Radial Flow Desiccant Dehumidification Bed," Applied Thermal Engineering, 28, 75-85.

Barlow, R. S. (1982) "Analysis of the Adsorption Process and of Desiccant cooling system- A Pseudo-steady-State Model for coupled Heat and Mass Transfer," Solar Energy Research Institute, SERI/TR-631-1330.

Dupont, M., Celestine, B., Nguyen, P.H, Merigoux, J., and Brandon, B. (1994) "Desiccant Solar Air Conditioning in Tropical Climates: I- Dynamic Experimental and Numerical Studies of Silica Gel and Activated Alumina," Solar Energy, 52, 6, 509-517.

Hamed, A. M. (2002) "Theoretical and Experimental Study on the Transient Adsorption Characteristics of a Vertical Packed Porous Bed," Renewable Energy, 27, 525-541.

Hamed. A. M. Abd-elrahman, W. R. and El-Emam, S. H. (2010) "Experimental study of the transient adsorption/desorption characteristics of silica gel particles in fluidized bed," Energy, 35, 6, 2468-2483.

Kabeel, A. E. (2009) "Adsorption–Desorption Operations of Multilayer Desiccant Packed Bed for Dehumidification Applications," Renewable Energy, 34, 255–265.

Pahwa, D. (1999) "Dehumidification - Desiccant Based," Air Conditioning and Refrigeration Journal, Vol. 2, No. 3.

Pesaran A. A. and Bingham C. E. (1989) "Testing of Novel Desiccant Materials and Dehumidifier Matrices for Desiccant Cooling Applications," SERI/TP-254-3478.

Pesaran, A.. A. (1993) "A Review of Desiccant Dehumidification Technology," National Renewable Energy Laboratory Golden, Colorado.

Rutherford T. R., (2000) "Desiccant Cooling Technology Resource Guide," U.S. Army Construction Engineering Research Laboratory.

Appendix

Isotherms for silica gel and activated alumina were studied by Dupont, M. *et al.*, (1994). For activated alumina, relative humidity at its surface RH^* was correlated to the alumina temperature T and its water content X as shown in equation (1).

$$\left.\begin{aligned} RH^* = {} & A_1.T.X^2 + A_2.T.X^3 + A_3.T.X^4 \\ & + A_4.T.X + A_5.T.X^5 + A_6.X^4 + \\ & A_7.X^3 + A_8.X^2 + A_9.X + A_{10}.T^3.X^2 \\ & + A_{11}.T^2.X + A_{12}.T^2.X^2 \end{aligned}\right\} \quad (A1)$$

Where,

T: activated alumina temperature in °C,

X: water content of activated alumina (kg/kg),

RH^*: the equilibrium relative humidity at alumina surface and

Using the following constants,

A_1 =0.83768451, A_2 =-7.68553638, A_3 =23.7146148, A_4 =0.01742458, A_5 =-24.956832, A_6 = 209.574569, A_7 =-184.782104, A_8 =53.00115967, A_9 = -2.5565977, A_{10} =0.00000029, A_{11}=-0.00029927, A_{12} =0.00063593

A tool which simplifies the determination of air properties in a graphic presentation of several interrelated air parameters brought together, Pahwa, (1999). The following standard psychrometric equations (Barlow,1982) are used in the present study to plot an extended version of the psychrometric chart, in which the dry bulb temperature reaches 100 °C.

$$RH = \frac{P_v}{P_{sat}} \quad (A2)$$

$$\omega = \frac{0.662 P_v}{P_{atm} - P_v} \quad (A3)$$

$$RH = \frac{P_{atm} \cdot \omega}{(0.622 + \omega) P_{sat}} \quad (A4)$$

$$P_{sat} = \exp\left[23.28199 - \frac{378082}{T+273} - \frac{225805}{(T+273)^2}\right] \quad (A5)$$

$$\left.\begin{aligned} h_a = {} & (1005.22 + 0.02615 \times T) \cdot T \\ & + \omega \cdot (2500800 + 1868 \times T) \end{aligned}\right\} \quad (A6)$$